

Production of ω and ϕ Mesons in Near-Threshold πN Reactions: Baryon Resonances and Validity of the OZI Rule

A.I. Titov^{a,b,*}, B. Kämpfer^{a,†}, B.L. Reznik^{c,‡}

^a *Forschungszentrum Rossendorf, PF 510119, 01314 Dresden, Germany*

^b *Bogolyubov Laboratory of Theoretical Physics, JINR, Dubna 141980, Russia*

^c *Far-Eastern State University, Sukhanova 9, Vladivostok 690090, Russia*

Abstract

Results of a combined analysis are presented for the production of ω and ϕ mesons in πN reactions in the near-threshold region using throughoutly a conventional "non-strange" dynamics based on such processes which are allowed by the non-ideal $\omega - \phi$ mixing. We show that strong interferences of the t (meson exchange) and s and u (nucleon and nucleon resonance) channels differ significantly in ω and ϕ production amplitudes. This leads to a decrease of the relative yields in comparison with expectations based on one-channel models with standard $\omega - \phi$ mixing. We find a strong and non-trivial difference between observables in ω and ϕ production reactions caused by the different role of the nucleon and nucleon resonance amplitudes. A series of predictions for the experimental study of this effect is presented.

PACS: 13.75.-n; 14.20.-c; 21.45.+v

keywords: hadron reactions; phi and omega production; threshold behavior.

I. INTRODUCTION

The present interest in a combined study of the ω and ϕ meson production in different elementary reactions is mainly related to the investigation of the hidden strangeness degrees of freedom in the nucleon. Since the ϕ meson is thought to consist mainly of strange quarks, its production should be suppressed according to the OZI rule [1] if the entrance channel does not possess a considerable admixture of strangeness. The standard OZI rule violation is described by the deviation from the ideal $\omega - \phi$ mixing by the angle $\Delta\theta_V \simeq 3.7^\circ$ [2], which

*E-mail address: atitov@thsun1.jinr.ru

†Corresponding author.

E-mail address: kaempfer@fz-rossendorf.de (B. Kämpfer).

‡E-mail address: reznik@dvgu.ru

is a measure of the small contribution of light u, \bar{u} and d, \bar{d} quarks in the ϕ meson, or strange s, \bar{s} quarks in the ω meson. Thus, the ratio of ω to ϕ production cross sections is expected to be $R_{\omega/\phi}^2 \simeq \text{ctg}^2 \Delta\theta_V \simeq 2.4 \times 10^2$.

Indeed, the recent experiments on the proton annihilation at rest (cf. [3] for references and a compilation of data) point to a large apparent violation of the OZI rule, which is interpreted [3,4] as a hint to an intrinsic $s\bar{s}$ component in the proton. However, the data can be explained as well by modified meson exchange models [5] without introducing any strangeness component in the nucleon or OZI rule violation mechanisms.

On the other hand, the analysis of the πN sigma term [6] suggests that the proton might contain a strange quark admixture as large as 20%. Thus this issue remains controversial. Therefore it is tempting to look for other observables [3,7,8] that are sensitive to the strangeness content of the nucleon. Most of them are related to a possible strong interference of delicate $s\bar{s}$ knock-out (or shake-off) amplitudes and the “non-strange” amplitude which is caused by OZI rule allowed processes, or by processes wherein the standard OZI rule violation comes from the $\phi - \omega$ mixing.

A detailed analysis of the current status of the OZI rule in πN and NN reactions has been presented recently in [9]. It is shown in [9] that existing data for the ω and ϕ meson production in πN reactions give for the ratio of averaged amplitudes the value of $R_{\omega/\phi} = 8.7 \pm 1.8$, which is much smaller than the standard OZI rule violation value of $R_{\omega/\phi}^{OZI} = 15.43$ and may be interpreted as a hint to non-zero strangeness components in the nucleon.

Obviously, reliable information on a manifestation of hidden strangeness in the combined study of ϕ and ω production processes can be obtained only when the conventional, i.e. non-exotic, amplitudes have been understood quantitatively. The reaction $\pi N \rightarrow VN$ with $V = \omega, \phi$ has the evident advantage to be a simple hadronic reaction representing a subprocess, e.g., in $NN \rightarrow VNN$ reactions. The study of the former reactions is one of the objectives of the present work. The dominant conventional processes are depicted in Fig. 1, where (a) is the t channel meson exchange process, while (b) depicts the s, u nucleon and nucleon resonance channels. When taking separately each of the amplitudes, the ratio of ω to ϕ production amplitudes is proportional to $\text{ctg} \Delta\theta_V = 15.43$ and the question arises how their coherent sum can result in a deviation from this value.

Note that most of the previous considerations of the possible violation of the OZI rule in hadronic reactions are based on one-channel models in the spirit of [10,11]. But if one assumes that the process is a coherent sum of at least two amplitudes, say for example, a meson exchange and a nucleon term, then the result may be different from the naive expectation. Indeed, let us suppose for a moment that, because of some hadronic dynamics, the nucleon term for the ϕ production is suppressed relative to the meson exchange term. Then the ratio of ω to ϕ amplitudes becomes

$$R_{\omega/\phi} = \text{ctg} \Delta\theta_V \frac{|1 + R_{N/M}^\omega|}{|1 + R_{N/M}^\phi|} \approx \text{ctg} \Delta\theta_V |1 + R_{N/M}^\omega|, \quad (1)$$

where $R_{N/M}^{\omega,\phi}$ are the ratios of nucleon and meson exchange amplitudes. Thus, one can get immediately an enhancement (suppression) of $R_{\omega/\phi}$, as compared to the OZI rule prediction, for a constructive (destructive) interference between the two ω amplitudes and for $|R_{N/M}^\phi| \ll$

$|R_{N/M}^\omega| < 1$. Our previous study [12] of ϕ production shows that the interference between meson exchange and nucleon terms is destructive. Assuming the same for ω production, $R_{\omega/\phi}$ must decrease, even without any speculation on a strangeness content in the nucleon. In case of considering the ω production, however, this two-channel model is by no means longer adequate, because one has to include various strong resonance channels. The ratio $R_{(N+N^*)/M}^\omega$ becomes complex which may change the above estimates in any direction.

The resonance contribution to vector meson production has its own interest because it might affect significantly in-medium polarization operators and the corresponding dilepton emissivity of hadronic matter [13–15]. Therefore its detailed study in elementary πN processes is another objective of the present work. An important step in this direction has been done recently by Riska and Brown in [16], where the relevant πNN^* , ωNN^* and ϕNN^* coupling constants are expressed in terms of the corresponding couplings to nucleons using a quark model. Our study here exploits essentially the findings of [16]. The role of the low-lying nucleon resonances in a combined study of ρ^0 and ω production based on the relativistic coupled-channel model has been studied in Refs. [14,17]. Some aspects of the ρ meson spectral function in the nucleon resonance model have been discussed in [18]. The contribution of the higher resonances to the ω photo-production has been analyzed in Ref. [19].

Our analysis of the reaction $\pi N \rightarrow VN$ is based on calculations of the diagrams in Fig. 1. While the diagrams in Fig. 1 look like usual Feynman diagrams it should be stressed that they give a guidance of how to obtain from an interaction Lagrangian of hadronic fields a covariant parameterization of observables in strict tree level approximation. Additional ingredients are needed to achieve an accurate description of data within such a framework. In particular, the vertices needs to be dressed by form factors. The early theoretical studies [20,21] show, indeed, that predictions for hadronic observables are very sensitive to the parameters of the form factors which can not be fixed unambiguously without adjustments relying on the corresponding experimental data.

In Refs. [22,23] the parameters of VNN interactions have been determined by analyzing commonly the reactions $pp \rightarrow pp\omega$ and $pp \rightarrow pp\phi$ and the corresponding new DISTO data [24] at a given beam energy assuming the same production mechanism without resonance contributions. In a previous paper [12], in order to constrain the parameter space further, we performed a combined analysis of the reactions $\pi^- p \rightarrow n\phi$ and $pp \rightarrow pp\phi$ at the same energy excess. A good description of available data has been achieved. We did not consider in [12] the ω production for which the production mechanism is more complicated because of the resonance contributions shown in Fig. 1b. Therefore, the problem of the validity of the OZI rule was beyond the scope of considerations in [12].

In this paper we attempt a different approach with the goal to check the validity of the OZI rule in a combined study of the related reactions $\pi N \rightarrow N\omega$ and $\pi N \rightarrow N\phi$ using the known data within the same interval of excess energies $10 \cdots 100$ MeV and taking into account the nucleon resonance channels.

Our paper is organized as follows. In Section II, we define the effective Lagrangians, derive expressions for the amplitudes of the processes shown in Fig. 1 and discuss the parameter fixing. In Section III the results of numerical calculations and predictions are presented. The summary is given in Section IV.

II. AMPLITUDES

The differential cross section of the reaction $\pi^- p \rightarrow V n$ with $V = \omega, \phi$ (cf. Fig. 1) has the obvious form in standard notation

$$\frac{d\sigma}{d\Omega} = \frac{1}{64\pi^2 s} \frac{|\mathbf{q}|}{|\mathbf{k}|} |T|^2, \quad (2)$$

where $k = (E_\pi, \mathbf{k})$ and $q = (E_V, \mathbf{q})$ are the four-momenta of the pion and the vector meson in the center of mass system (c.m.s.); the squared invariant amplitude $|T|^2$ includes the average and sum over the initial and final spin states, respectively. We denote the four-momenta of the initial (target) and final (recoil) nucleons by p and p' ; Ω and θ are the solid and polar angles of the produced vector meson in the c.m.s.; $s = (p + k)^2$ is the usual Mandelstam variable.

We also consider the spin density matrix $\rho_{rr'}$ which defines the angular distribution in the decays $\omega, \phi \rightarrow e^+ e^-$, $\omega \rightarrow \pi^+ \pi^- \pi^0$ and $\phi \rightarrow K^+ K^-$. It has a simple form in the system where the vector meson is at rest (for details see [12]). The decay angles Θ, Φ are defined as polar and azimuthal angles of the direction of the three-momentum of one of the decay particles in the vector meson's rest frame. For the $\omega \rightarrow \pi^+ \pi^- \pi^0$ decay, Θ is the polar angle of the direction of the vector product $[\mathbf{k}_{\pi^+} \times \mathbf{k}_{\pi^-}]$, where \mathbf{k}_{π^+} and \mathbf{k}_{π^-} are the momenta of π^+ and π^- mesons, respectively [25]. The $e^+ e^-$ decay distribution integrated over the azimuthal angle Φ , $\mathcal{W}(\cos \Theta)$, depends only on the diagonal matrix elements ρ_{00} , $\rho_{11} = \rho_{-1-1}$, normalized as $\rho_{00} + 2\rho_{11} = 1$, according to

$$\mathcal{W}^{e^+ e^-}(\cos \Theta) = \frac{3}{4} [1 + \rho_{00} + (1 - 3\rho_{00}) \cos^2 \Theta]. \quad (3)$$

The corresponding distributions for the hadronic decays $\phi \rightarrow K^+ K^-$, $\omega \rightarrow \pi^+ \pi^- \pi^0$ are

$$\mathcal{W}^h(\cos \Theta) = \frac{3}{2} [1 - \rho_{00} - (1 - 3\rho_{00}) \cos^2 \Theta]. \quad (4)$$

In our calculation we choose the quantization axis \mathbf{z} along the beam momentum.

A. Effective Lagrangians

In calculating the invariant amplitudes for the basic processes shown in Fig. 1 we use the following effective interaction Lagrangians.

(i) interactions in the meson exchange process (Fig. 1a):

$$\mathcal{L}_{V\rho\pi} = g_{V\rho\pi} \epsilon^{\mu\nu\alpha\beta} \partial_\mu^{(V)} V_\nu \text{Tr}(\partial_\alpha \rho_\beta \pi), \quad (5)$$

$$\mathcal{L}_{\rho NN} = -g_{\rho NN} \bar{\psi}_N \left(\gamma_\mu - \frac{\kappa_{\rho NN}}{2M_N} \sigma_{\mu\nu} \partial_{(\rho)}^\nu \right) \rho^\mu \psi_N, \quad (6)$$

where $\text{Tr}(\rho\pi) = \rho^0 \pi^0 + \rho^+ \pi^- + \rho^- \pi^+$, and π and ρ^μ denote the pion and rho meson fields. The partial derivatives $\partial_\mu^{(V)}$ and $\partial_{(\rho)}^\nu$ are meant to act only on the corresponding fields V^μ and ρ^μ ; $\epsilon^{\mu\nu\alpha\beta}$ is the Levi-Civita symbol.

(ii) interactions in the baryonic channels (Fig. 1b):

$$\mathcal{L}_{MNN}^{N_{\frac{1}{2}}+(940)N} = \bar{\psi}_N \left[-\frac{f_{\pi NN}}{m_\pi} \gamma_5 \gamma_\mu \partial^\mu \boldsymbol{\pi} \cdot \boldsymbol{\tau} - g_{VNN} \left(\gamma_\mu - \frac{\kappa_{VNN}}{2M_N} \sigma_{\mu\nu} \partial^\nu \right) V^\mu \right] \psi_N, \quad (7)$$

$$\mathcal{L}_{MNN^*}^{N_{\frac{1}{2}}+(1440)P_{11}} = \bar{\psi}_N \left[-\frac{f_{\pi NN^*}^{1440}}{m_\pi} \gamma_5 \gamma_\mu \partial^\mu \boldsymbol{\pi} \cdot \boldsymbol{\tau} - g_{VNN^*}^{1440} (\gamma_\mu + \partial_\mu \not{\partial} m_V^{-2}) V^\mu \right] \psi_{N^*} + \text{h.c.}, \quad (8)$$

$$\mathcal{L}_{MNN^*}^{N_{\frac{3}{2}}-(1520)D_{13}} = \bar{\psi}_N \left[i \frac{f_{\pi NN^*}^{1520}}{m_\pi} \gamma_5 \partial^\alpha \boldsymbol{\pi} \cdot \boldsymbol{\tau} + \frac{g_{VNN^*}^{1520}}{m_V^2} \sigma_{\mu\nu} \partial^\nu \partial^\alpha V^\mu \right] \psi_{N^* \alpha} + \text{h.c.}, \quad (9)$$

$$\mathcal{L}_{MNN^*}^{N_{\frac{1}{2}}-(1535)S_{11}} = \bar{\psi}_N \left[-\frac{f_{\pi NN^*}^{1535}}{m_\pi} \gamma_\mu \partial^\mu \boldsymbol{\pi} \cdot \boldsymbol{\tau} - g_{VNN^*}^{1535} \gamma_5 (\gamma_\mu + \partial_\mu \not{\partial} m_V^{-2}) V^\mu \right] \psi_{N^*} + \text{h.c.}, \quad (10)$$

$$\mathcal{L}_{MNN^*}^{N_{\frac{1}{2}}-(1650)S_{11}} = \bar{\psi}_N \left[-\frac{f_{\pi NN^*}^{1650}}{m_\pi} \gamma_\mu \partial^\mu \boldsymbol{\pi} \cdot \boldsymbol{\tau} - g_{VNN^*}^{1650} \gamma_5 (\gamma_\mu + \partial_\mu \not{\partial} m_V^{-2}) V^\mu \right] \psi_{N^*} + \text{h.c.}, \quad (11)$$

$$\mathcal{L}_{MNN^*}^{N_{\frac{5}{2}}-(1675)D_{15}} = \bar{\psi}_N \left[-\frac{f_{\pi NN^*}^{1675}}{m_\pi^2} \partial^\alpha \partial^\beta \boldsymbol{\pi} \cdot \boldsymbol{\tau} + \frac{g_{VNN^*}^{1675}}{m_V^2} \epsilon^{\alpha\gamma\mu\nu} \gamma_\nu \partial_\gamma \partial^\beta V_\mu \right] \psi_{N^* \alpha\beta} + \text{h.c.}, \quad (12)$$

$$\begin{aligned} \mathcal{L}_{MNN^*}^{N_{\frac{5}{2}}+(1680)F_{15}} = \bar{\psi}_N & \left[-i \frac{f_{\pi NN^*}^{1680}}{m_\pi^2} \gamma_5 \partial^\alpha \partial^\beta \boldsymbol{\pi} \cdot \boldsymbol{\tau} \right. \\ & \left. + \frac{g_{VNN^*}^{1680}}{m_V^2} (\gamma_\mu + \partial_\mu \not{\partial} m_V^{-2}) \partial^\alpha \partial^\beta V^\mu \right] \psi_{N^* \alpha\beta} + \text{h.c.}, \end{aligned} \quad (13)$$

$$\mathcal{L}_{MNN^*}^{N_{\frac{3}{2}}-(1700)D_{13}} = \bar{\psi}_N \left[i \frac{f_{\pi NN^*}^{1700}}{m_\pi} \gamma_5 \partial^\alpha \boldsymbol{\pi} \cdot \boldsymbol{\tau} + \frac{g_{VNN^*}^{1700}}{m_V^2} \sigma_{\mu\nu} \partial^\nu \partial^\alpha V^\mu \right] \psi_{N^* \alpha} + \text{h.c.}, \quad (14)$$

$$\begin{aligned} \mathcal{L}_{MNN^*}^{N_{\frac{3}{2}}-(1720)P_{13}} = \bar{\psi}_N & \left[i \frac{f_{\pi NN^*}^{1720}}{m_\pi} \partial^\alpha \boldsymbol{\pi} \cdot \boldsymbol{\tau} \right. \\ & \left. - \frac{g_{VNN^*}^{1720}}{M_{N^*} + M_N} \gamma_5 (\gamma_\mu \partial^\alpha - g_\mu^\alpha \not{\partial}) V^\mu \right] \psi_{N^* \alpha} + \text{h.c.}, \end{aligned} \quad (15)$$

where $\boldsymbol{\pi}$, V_μ , ψ_N and ψ_{N^*} are the pion iso-vector, iso-scalar vector meson $V = \omega, \phi$, nucleon and Rarita-Schwinger nucleon resonances field operators, respectively, and the subscript M stands for "meson". $\boldsymbol{\tau}$ denotes the Pauli matrix. Note that these interaction Lagrangians do not contain partial derivatives of the fields ψ_{\dots} and their adjoints $\bar{\psi}_{\dots}$. The notation of the masses is self-explaining. We use the convention of Bjorken and Drell [26] in definitions of γ matrices and the spin matrix $\sigma_{\mu\nu}$. The expressions Eqs. (7 - 15) are based on [16].¹ As in [16] we include here all **** resonances up to 1720 MeV according to [2] and the *** resonance $N_{\frac{3}{2}}-(1700)D_{13}$ as well. The contribution of the *** resonance $N_{\frac{1}{2}}-(1710)P_{13}$ will be discussed below.

All coupling constants with off-shell mesons are dressed by monopole form factors [27] $F_i = (\Lambda_i^2 - m_i^2)/(\Lambda_i^2 - k_i^2)$, where k_i is the four-momentum of the exchanged meson. Following the scheme of the meson photo-production in [28] we assume that the VNN and VNN^* vertices must be dressed by form factors for off-shell baryons

¹ Our notation differs from that in [16] by the substitutions $\partial \rightarrow i\partial$ and $ig_{VNN} \rightarrow -g_{VNN}$ keeping the relative phases between $f_{\pi NN}$ and $f_{\pi NN^*}$ and g_{VNN} and g_{VNN^*} the same as in [16]. We also express \mathcal{L}_{MNN^*} in a manifestly gauge-invariant form.

$$F_B(r^2) = \frac{\Lambda_B^4}{\Lambda_B^4 + (r^2 - M_B^2)^2}, \quad (16)$$

where M_B is the baryon mass and r is the four-momentum of the virtual baryons $B = N, N^*$ in Fig. 1b.

B. Invariant amplitudes

The total invariant amplitude is sum of the meson exchange, nucleon and nucleon resonance channels,

$$T_\lambda = T_\lambda^{(M)} + T_\lambda^{(N)} + T_\lambda^{(N^*)}, \quad (17)$$

where $\lambda = 0, \pm 1$ is the polarization projection of the produced vector meson. The amplitude for the meson exchange channel in Fig. 1a reads

$$T_\lambda^{(M)} = K^{\pi N} \epsilon^{\alpha\beta\gamma\delta} [\bar{u}(p') \Gamma_\delta^{(\rho)}(k_{(\rho)}) u(p)] q_\alpha k_\gamma \epsilon_\beta^{*\lambda} I_\pi, \quad (18)$$

where

$$\Gamma_\alpha^{(\rho)}(k_{(\rho)}) = \gamma_\alpha + i \frac{\kappa_{\rho NN}}{2M_N} \sigma_{\alpha\beta} k_{(\rho)}^\beta, \quad (19)$$

$$K^{\pi N}(k_{(\rho)}) = -\frac{g_{\rho NN} g_{V\rho\pi} \Lambda_{\rho NN}^2 - m_\rho^2 \Lambda_{V\rho\pi}^2 - m_\rho^2}{k_{(\rho)}^2 - m_\rho^2 \Lambda_{\rho NN}^2 - k_{(\rho)}^2 \Lambda_{V\rho\pi}^2 - k_{(\rho)}^2} \quad (20)$$

with $k_{(\rho)} = p' - p$ as the virtual ρ meson's four-momentum; ϵ_β^λ is the vector meson's polarization four-vector, I_π denotes the isospin factor being $\sqrt{2}$ (1) for a π^- (π^0) meson in the entrance channel; the nucleon spin indices are not displayed; $\alpha, \beta, \gamma, \delta, \mu, \nu, \tau$ are Lorentz indices throughout the paper (not to be mixed with the notations of meson species π, ρ, ω, ϕ), and $u(p)$ denotes bispinors (not to be mixed with the Mandelstam variable u).

The invariant amplitudes for the nucleon and resonant channels in Fig. 1b have the following form

$$T_\lambda^{(N)} = g_{VNN} \frac{f_{\pi NN}}{m_\pi} \bar{u}(p') \mathcal{A}^\mu(N) u(p) \epsilon_\mu^{*\lambda} I_\pi, \quad (21)$$

$$T_\lambda^{(N^*)} = g_{VNN^*} \frac{f_{\pi NN^*}}{m_\pi} \bar{u}(p') \mathcal{A}^\mu(N^*) u(p) \epsilon_\mu^{*\lambda} I_\pi, \quad (22)$$

where the operators $\mathcal{A}_\mu(N)$ and $\mathcal{A}_\mu(N^*)$ follow from the effective Lagrangians of Eqs. (7 - 15) as

$$\mathcal{A}_\mu(N^{940}) = i \frac{\Gamma_\mu^V(-q) \Lambda(p_L, M_{N^*}) \gamma_5 \not{k} F_N(s)}{s - m_N^2} + i \frac{\gamma_5 \not{k} \Lambda(p_R, M_{N^*}) \Gamma_\mu^V(-q) F_N(u)}{u - m_N^2}, \quad (23)$$

$$\mathcal{A}_\mu(N^{1440}) = i \frac{\gamma_\mu \Lambda(p_L, M_{N^*}) \gamma_5 \not{k} F_{N^*}(s)}{s - M_{N^*}^2 + i\Gamma_{N^*} M_{N^*}} + i \frac{\gamma_5 \not{k} \Lambda(p_R, M_{N^*}) \gamma_\mu F_{N^*}(u)}{u - M_{N^*}^2 + i\Gamma_{N^*} M_{N^*}}, \quad (24)$$

$$\mathcal{A}_\mu(N^{1520}) = -\frac{\sigma_{\mu\nu}q^\nu q^\alpha \Lambda_{\alpha\beta}(p_L, M_{N^*}) \gamma_5 k^\beta F_{N^*}(s)}{m_V^2(s - M_{N^*}^2 + i\Gamma_{N^*} M_{N^*})} - \frac{\gamma_5 k^\alpha \Lambda_{\alpha\beta}(p_R, M_{N^*}) \sigma_{\mu\nu} q^\nu q^\beta F_{N^*}(u)}{m_V^2(u - M_{N^*}^2 + i\Gamma_{N^*} M_{N^*})}, \quad (25)$$

$$\mathcal{A}_\mu(N^{1535}) = i\frac{\gamma_5 \gamma_\mu \Lambda(p_L, M_{N^*}) \not{k} F_{N^*}(s)}{s - M_{N^*}^2 + i\Gamma_{N^*} M_{N^*}} + i\frac{\not{k} \Lambda(p_R, M_{N^*}) \gamma_5 \gamma_\mu F_{N^*}(u)}{u - M_{N^*}^2 + i\Gamma_{N^*} M_{N^*}}, \quad (26)$$

$$\mathcal{A}_\mu(N^{1650}) = i\frac{\gamma_5 \gamma_\mu \Lambda(p_L, M_{N^*}) \not{k} F_{N^*}(s)}{s - M_{N^*}^2 + i\Gamma_{N^*} M_{N^*}} + i\frac{\not{k} \Lambda(p_R, M_{N^*}) \gamma_5 \gamma_\mu F_{N^*}(u)}{u - M_{N^*}^2 + i\Gamma_{N^*} M_{N^*}}, \quad (27)$$

$$\mathcal{A}_\mu(N^{1675}) = -\frac{\epsilon_{\tau\mu\nu}^{\alpha} q^\tau q^\beta k^\gamma k^\delta}{m_\pi m_V^2} \left(\frac{\gamma^\nu \Lambda_{\alpha\beta, \gamma\delta}(p_L, M_{N^*}) F_{N^*}(s)}{s - M_{N^*}^2 + i\Gamma_{N^*} M_{N^*}} + \frac{\Lambda_{\gamma\delta, \alpha\beta}(p_R, M_{N^*}) \gamma^\nu F_{N^*}(u)}{u - M_{N^*}^2 + i\Gamma_{N^*} M_{N^*}} \right), \quad (28)$$

$$\mathcal{A}_\mu(N^{1680}) = -i\frac{q^\alpha q^\beta k^\gamma k^\delta}{m_\pi m_V^2} \left(\frac{\gamma_\mu \Lambda_{\alpha\beta, \gamma\delta}(p_L, M_{N^*}) \gamma_5 F_{N^*}(s)}{s - M_{N^*}^2 + i\Gamma_{N^*} M_{N^*}} + \frac{\gamma_5 \Lambda_{\gamma\delta, \alpha\beta}(p_R, M_{N^*}) F_{N^*}(u)}{u - M_{N^*}^2 + i\Gamma_{N^*} M_{N^*}} \right), \quad (29)$$

$$\mathcal{A}_\mu(N^{1700}) = -\frac{\sigma_{\mu\nu}q^\nu q^\alpha \Lambda_{\alpha\beta}(p_L, M_{N^*}) \gamma_5 k^\beta F_{N^*}(s)}{m_V^2(s - M_{N^*}^2 + i\Gamma_{N^*} M_{N^*})} - \frac{\gamma_5 k^\alpha \Lambda_{\alpha\beta}(p_R, M_{N^*}) \sigma_{\mu\nu} q^\nu q^\beta F_{N^*}(u)}{m_V^2(u - M_{N^*}^2 + i\Gamma_{N^*} M_{N^*})}, \quad (30)$$

$$\mathcal{A}_\mu(N^{1720}) = i\frac{\gamma_5 (q^\alpha \gamma_\mu - g_\mu^\alpha \not{q}) \Lambda_{\alpha\beta}(p_L, M_{N^*}) k^\beta F_{N^*}(s)}{(M_{N^*} + M_N)(s - M_{N^*}^2 + i\Gamma_{N^*} M_{N^*})} + i\frac{k^\beta \Lambda_{\beta\alpha}(p_R, M_{N^*}) \gamma_5 (q^\alpha \gamma_\mu - g_\mu^\alpha \not{q}) F_{N^*}(u)}{(M_{N^*} + M_N)(u - M_{N^*}^2 + i\Gamma_{N^*} M_{N^*})}, \quad (31)$$

with $p_L = p + k$, $p_R = p - q$ and Γ_μ^V as in Eq. (19) but with κ_{VNN} .

The resonance propagators in Eqs. (24 - 31) are defined by the conventional method [29] assuming the validity of the spectral decomposition

$$\psi_{N^*}(x) = \int \frac{d^3\mathbf{p}}{(2\pi)^3 \sqrt{2E_p}} \left[a_{\mathbf{p},r} u_{N^*}^r(p) e^{-ipx} + b_{\mathbf{p},r}^+ v_{N^*}^r(p) e^{+ipx} \right]. \quad (32)$$

The finite decay width Γ_{N^*} is introduced into the propagator denominators by substituting $M_{N^*} \rightarrow M_{N^*} + \frac{1}{2}\Gamma_{N^*}$. Therefore, the operators $\Lambda(p, M)$ are defined as

$$\Lambda(p, M) = \frac{1}{2} \sum_r \left(\left(1 + \frac{p_0}{E_0}\right) u^r(\mathbf{p}, E_0) \otimes \bar{u}^r(\mathbf{p}, E_0) - \left(1 - \frac{p_0}{E_0}\right) v^r(-\mathbf{p}, E_0) \otimes \bar{v}^r(-\mathbf{p}, E_0) \right) = \not{p} + M, \quad (33)$$

$$\Lambda_{\alpha\beta}(p, M) = \frac{1}{2} \sum_r \left(\left(1 + \frac{p_0}{E_0}\right) \mathcal{U}_\alpha^r(\mathbf{p}, E_0) \otimes \bar{\mathcal{U}}_\beta^r(\mathbf{p}, E_0) - \left(1 - \frac{p_0}{E_0}\right) \mathcal{V}_\alpha^r(-\mathbf{p}, E_0) \otimes \bar{\mathcal{V}}_\beta^r(-\mathbf{p}, E_0) \right), \quad (34)$$

$$\Lambda_{\alpha\beta,\gamma\delta}(p, M) = \frac{1}{2} \sum_r \left(\left(1 + \frac{p_0}{E_0}\right) \mathcal{U}_{\alpha\beta}^r(\mathbf{p}, E_0) \otimes \bar{\mathcal{U}}_{\gamma\delta}^r(\mathbf{p}, E_0) - \left(1 - \frac{p_0}{E_0}\right) \mathcal{V}_{\alpha\beta}^r(-\mathbf{p}, E_0) \otimes \bar{\mathcal{V}}_{\gamma\delta}^r(-\mathbf{p}, E_0) \right), \quad (35)$$

where $E_0 = \sqrt{\mathbf{p}^2 + M^2}$, and the Rarita-Schwinger spinors read

$$\mathcal{U}_\alpha^r(p) = \sum_{\lambda,s} \langle 1 \lambda \frac{1}{2} s | \frac{3}{2} r \rangle \varepsilon_\alpha^\lambda(p) u^s(p), \quad (36)$$

$$\mathcal{U}_{\alpha\beta}^r(p) = \sum_{\lambda,\lambda',s,t} \langle 1 \lambda \frac{1}{2} s | \frac{3}{2} t \rangle \langle \frac{3}{2} t 1 \lambda' | \frac{5}{2} r \rangle \varepsilon_\alpha^\lambda(p) \varepsilon_\beta^{\lambda'}(p) u^s(p). \quad (37)$$

The spinors v and \mathcal{V} are related to u and \mathcal{U} as $v(p) = i\gamma_2 u^*(p)$ and $\mathcal{V}(p) = i\gamma_2 \mathcal{U}^*(p)$, respectively.

The polarization four-vector for a spin-1 particle with spin projection λ , four-momentum $p = (E, \mathbf{p})$ and mass m_V reads

$$\varepsilon^\lambda(p) = \left(\frac{\boldsymbol{\epsilon}^\lambda \cdot \mathbf{p}}{m_V}, \frac{\mathbf{p} (\boldsymbol{\epsilon}^\lambda \cdot \mathbf{p})}{m_V(E + m_V)} \right), \quad (38)$$

where the three-dimensional polarization vector $\boldsymbol{\epsilon}$ is defined as

$$\boldsymbol{\epsilon}^{\pm 1} = \mp \frac{1}{\sqrt{2}} (1, \pm i, 0) \quad \boldsymbol{\epsilon}^0 = (0, 0, 1). \quad (39)$$

In our calculations we use energy-dependent total resonance decay widths Γ_{N^*} . However, taking into account that the effect of a finite width is quite different for s and u channels, because of the evident relation $|u| + M_{N^*}^2 \gg |s - M_{N^*}^2|$, we use $\Gamma_{N^*} = \Gamma_{N^*}^0$ for the u channels and

$$\Gamma_{N^*} = \Gamma_{N^*}^0 \left[1 - B_{N^*}^\pi + B_{N^*}^\pi \left(\frac{\mathbf{k}}{\mathbf{k}_0} \right)^{2J} \right], \quad (40)$$

for the s channels, where $\Gamma_{N^*}^0$ is the total on-shell resonance decay width and $B_{N^*}^\pi$ stands for the branching ratio of the $N^* \rightarrow N\pi$ decay channel taken from [2]; \mathbf{k}_0 is the pion momentum at the resonance position, i.e. at $\sqrt{s} = M_{N^*}$, and the factor $(\mathbf{k}/\mathbf{k}_0)^{2J}$ comes from a direct calculation of the $N^* \rightarrow N\pi$ decay width using the effective Lagrangians of Eqs. (8 - 15), where we keep the leading term proportional to \mathbf{k}^{2J} . Note, that the effect of the energy dependent finite decay width is more essential in near-threshold ω production for the higher resonances $N_{\frac{3}{2}-}(1700)D_{13}$ and $N_{\frac{3}{2}-}(1720)P_{13}$, where $|s - M_{N^*}^2| \sim \Gamma_{N^*} M_{N^*}$, but even there it becomes not so important because, as we will see, the contribution of these resonances to the total amplitude is rather small. Nevertheless, for completeness, we use the above prescription for all eight considered resonances.

C. Fixing parameters

The coupling constant $g_{\phi\rho\pi}$ is determined by the $\phi \rightarrow \rho\pi$ decay. The value $\Gamma_{\phi \rightarrow \rho\pi} = 0.69$ MeV [2] results in $|g_{\phi\rho\pi}| = 1.1 \text{ GeV}^{-1}$. The SU(3) symmetry considerations [23,30] predict a negative value for it. Thus $g_{\phi\rho\pi} = -1.1 \text{ GeV}^{-1}$.

The coupling constant $g_{\omega\rho\pi}$ is determined by the $\omega \rightarrow \gamma\pi$ decay. Relying on the vector dominance model one gets $g_{\omega\rho\pi} = 12.9 \text{ GeV}^{-1}$ [9].

The remaining parameters of the meson exchange amplitude for the process in Fig. 1a are taken from the Bonn model as listed in Table B.1 (Model II) of Ref. [27]: $g_{\rho NN} = 3.72$, $\kappa_{\rho NN} = 6.1$, and $\Lambda_{\rho NN} = 1.3$. The parameter $\Lambda_{V\rho\pi}^{\rho}$ will be determined later.

The nucleon and nucleon resonance amplitudes in Fig. 1b and Eqs. (23 - 31) are determined by the couplings $f_{\pi NN}$, $f_{\pi NN^*}$, $g_{\omega NN}$, $g_{\omega NN^*}$, $g_{\phi NN}$, $g_{\phi NN^*}$, $g_{V NN}\kappa_{V NN}$, the resonance widths $\Gamma_{N^*}^0$, the branching ratios $B_{N^*}^{\pi}$, and the cut-offs Λ_B . For the coupling constant $f_{\pi NN}$ we use the standard value $f_{\pi NN} = 1.0$ [16,27]. For the ωNN coupling we use the value $g_{\omega NN} = 10.35$ determined recently [31] by fitting the nucleon-nucleon scattering data. This value as well as $\kappa_{\omega NN} = 0$ is close to the one which has been found in a study of πN scattering and the reaction $\gamma N \rightarrow \pi N$ [32].

The values of coupling constants $f_{\pi NN^*}$ are determined from a comparison of calculated decay widths $\Gamma_{N^* \rightarrow N\pi}$ with the corresponding experimental values [2]. The corresponding signs are taken in accordance with the quark model prediction of Ref. [16].

The values of coupling constants $g_{\omega NN^*}$ are found as $g_{\omega NN^*} = [g_{\omega NN^*}/g_{\omega NN}]g_{\omega NN}$, where the ratio $[g_{\omega NN^*}/g_{\omega NN}]$ is determined by the quark model calculation of Ref. [16]. For convenience we show all the coupling constants, decay widths and branching ratios used in our calculation in Table 1. The masses, decay widths and branching ratios in Table 1 represent the averages in [2]. Slightly different values have been extracted in [33] in a recent reanalysis of the data.

The couplings ϕNN , ϕNN^* determined by SU(3) symmetry considerations are

$$g_{\phi NN} = -\text{tg}\Delta\theta_V g_{\omega NN}, \quad g_{\phi NN^*} = -\text{tg}\Delta\theta_V g_{\omega NN^*}, \quad (41)$$

where $\Delta\theta_V \simeq 3.7^{\circ}$ is the deviation from the ideal $\omega - \phi$ mixing. Similarly, we assume $g_{\phi NN}\kappa_{\phi NN} \simeq -\text{tg}\Delta\theta_V g_{\omega NN}\kappa_{\omega NN} = 0$, or $\kappa_{\phi NN} \simeq 0$, which is consistent with the estimate in [34].

The yet undetermined parameters are: the cut-off parameters $\Lambda_{\phi\rho\pi}^{\rho}$ and $\Lambda_{\omega\rho\pi}^{\rho}$ for the virtual ρ meson in the $V\rho\pi$ vertex, the cut-off Λ_N and the eight cut-offs Λ_{N^*} in Eq. (16). We can reduce the number of parameters by making the natural assumptions

$$\Lambda_{\phi\rho\pi}^{\rho} = \Lambda_{\omega\rho\pi}^{\rho} \equiv \Lambda_V^{\rho}, \quad (42)$$

$$\Lambda_N = \Lambda_{N^*} \equiv \Lambda_B. \quad (43)$$

Our best fit of total cross sections of existing data is obtained by $\Lambda_V^{\rho} = 1.24 \text{ GeV}$ and $\Lambda_B = 0.66 \text{ GeV}$.

III. RESULTS

The results of our full calculation of the total cross sections as a function of the energy excess $\Delta s^{1/2} = \sqrt{s} - M_N - m_V$, including all amplitudes depicted in Fig. 1, are represented by the solid curves in Fig. 2. We also show separately the contributions of meson exchange, nucleon and nucleon resonance channels. The data for the reaction $\pi^- p \rightarrow \phi n$ are taken from Ref. [35], while the data for the reactions $\pi^+ n \rightarrow \omega p$ and $\pi^- p \rightarrow \omega n$ are from Refs. [35,36], respectively. Note that here we display the total cross section of the reaction $\pi^- p \rightarrow \omega n$, σ_{tot} , which differs from the differential cross section σ_{dif} in Ref. [36] by a factor [9,37] included in the phase space of the unstable ω meson,

$$\sigma_{\text{tot}} = \sigma_{\text{dif}} \left\{ \frac{\int_{\sqrt{P_{\text{min}}^2 + M_N^2}}^{\sqrt{P_{\text{max}}^2 + M_N^2}} \sqrt{\frac{\lambda_f(s')\lambda_i(s)}{\lambda_f(s)\lambda_i(s')}} \frac{2\sqrt{s'}\Gamma_\omega m_\omega dE}{\pi((m_\omega^2 - s' + 2\sqrt{s'}E - M_N^2)^2 + \Gamma_\omega^2 m_\omega^2)}} \right\}^{-1}, \quad (44)$$

where $\sqrt{s'} = E + \sqrt{E^2 - M_N^2 + m_\omega^2}$, Γ_ω is the ω decay width and $\lambda_i(s)$ ($\lambda_f(s)$) = $\lambda(s, m_\pi^2, M_N^2)$ ($\lambda(s, m_\omega^2, M_N^2)$) with $\lambda(x, y, z) = (x - y - z)^2 - 4yz$. The intervals $[P_{\text{max}}, P_{\text{min}}]$ for given p' (or s) are as in [36].

From Fig. 2 (left panel) it is evident that the total amplitude of ω production is a result of strong interferences of all channels: the meson exchange (dot-dashed curve), the nucleon term (long dashed curve) and the resonance contribution (dashed curve) play a comparative role. For the ϕ production (cf. Fig. 2, right panel) only meson and nucleon terms are important. The resonance contribution is rather small and is therefore not displayed here. Moreover the relative contribution of the nucleon term in ϕ production is much smaller than for ω production. That is because the initial energy $\sqrt{s} = M_N + m_V + \Delta s^{1/2}$ is greater for the ϕ production at the same energy excess and as a consequence, we have two suppression factors: (i) the nucleon/resonance denominators and (ii) the form factors F_{N,N^*} in Eqs. (23 - 31). The interference of the meson exchange and nucleon terms is almost destructive, while the contribution of the resonant part is more complicated because the amplitude is complex with different phases for different resonances.

In order to illustrate the structure of the resonant part we show in Fig. 3 the contribution of each resonance separately as a function of the ω production angle at two excess energies $\Delta s^{1/2} = 20$ (100) MeV at left (right) panel. One can see that just near the threshold the resonances with $J = \frac{1}{2}$ are important. Together with the nucleon term they are $N_{\frac{1}{2}^+}(1440)P_{11}$, $N_{\frac{1}{2}^-}(1535)S_{11}$ and $N_{\frac{1}{2}^-}(1650)S_{11}$. It is interesting that the separate contributions of the two latter ones are greater than the nucleon term. But their phases are opposite and, therefore, they cancel each other. The cancellation increases with energy which results in a total decrease of the resonance contribution. On the other hand one can see that the relative role of the higher spin resonances with orbital/radial excitations, being proportional to \mathbf{q}^2 and \mathbf{q}^4 , increases with increasing values of $\Delta s^{1/2}$, as illustrated in Fig. 4. This enhancement, however, is smaller than the effect of the strong destructive interference of the resonance amplitudes and, therefore, the total contribution of the resonance channel decreases with energy as shown in Fig. 2.

In our analyses we do not include the *** resonance $N_{\frac{1}{2}^+}(1710)P_{11}$ [2], as in [16]. A simple estimate shows that its contribution is rather small. Indeed, the calculation in [15], within the vector dominance model, shows that the ωNN^* coupling for $N_{\frac{1}{2}^+}(1710)P_{11}$ is about four times smaller than for the $N_{\frac{1}{2}^+}(1440)P_{11}$ resonance. Observing further that the corresponding pion decay width of $N_{\frac{1}{2}^+}(1710)P_{11}$, $5 \cdot \cdot 15$ MeV, is much smaller than that of $N_{\frac{1}{2}^+}(1440)P_{11}$, $210 \cdot \cdot 250$ MeV, we can expect a negligible contribution of $N_{\frac{1}{2}^+}(1710)P_{11}$ being about one order of magnitude smaller than the one of $N_{\frac{1}{2}^+}(1440)P_{11}$.

Figs. 5 and 6 show the angular distributions of the ω and ϕ production cross sections at $\Delta s^{1/2} = 20$ and 100 MeV, respectively. One can see that the destructive interference between meson exchange and nucleon channels, which is stronger for backward production, results in a non-monotonic angular distribution. The effect is stronger at $\Delta s^{1/2} = 100$ MeV.

Fig. 7 (left panel) shows the ratio of the averaged amplitudes $|T_V|$ of ω and ϕ production as a function of the vector meson's production angle at $\Delta s^{1/2} = 20$ MeV. $|T_V|$ is defined by

$$|T_V| = \left[\sum_{m_i, m_f, \lambda} |T_{m_f, \lambda; m_i}^V|^2 \right]^{\frac{1}{2}}, \quad (45)$$

where m_i, m_f, λ are the spin projection of target, recoil protons and vector meson, respectively. The dotted straight lines in Fig. 7 correspond to the standard OZI rule violation value $R_{\omega/\phi}^{OZI} = \text{ctg} \Delta \theta_V = 15.43$. The long dashed curve corresponds to the ratio of pure nucleon channels taken separately, the dot-dashed curve is result for a pure meson exchange, while the solid line represents the full calculation. Note that the ratio even for pure meson exchange amplitudes $R_{\omega/\phi}^M$ is smaller than $R_{\omega/\phi}^{OZI}$. That is because at the threshold

$$R_{\omega/\phi}^M \simeq \frac{g_{\omega\rho\pi}}{g_{\phi\rho\pi}} \frac{m_\omega}{m_\phi} \frac{f(m_\omega)}{f(m_\phi)} \simeq 9.9 \frac{f(m_\omega)}{f(m_\phi)}, \quad (46)$$

where $f(m)$ is a smooth function of m . The ratio for pure resonance terms is greater than $R_{\omega/\phi}^{OZI}$ by an order of magnitude and more, i.e., $R_{\omega/\phi}^{N^*} \sim 500$ (250) at $\theta = \pi$ (0), because of a strong propagator and form factor suppression for ϕ production. In the absence of the resonant amplitude the destructive interference of meson exchange (M) and nucleon (N) channels results in $R_{\omega/\phi}^{M+N} < R_{\omega/\phi}^M$. The presence of the resonance components leads to $R_{\omega/\phi}^M < R_{\omega/\phi} < R_{\omega/\phi}^{OZI}$.

Fig. 7 (right panel) shows the ratio of the angular integrated amplitudes

$$\langle |T_V| \rangle_\Omega = \left[\sum_{m_i, m_f, \lambda} \frac{1}{4\pi} \int d\Omega |T_{m_f, \lambda; m_i}^V|^2 \right]^{\frac{1}{2}} \quad (47)$$

of ω and ϕ production as a function of $\Delta s^{1/2}$. One can see that $R_{\omega/\phi}$ (solid curve) may be slightly above or below the pure $R_{\omega/\phi}^M$ value (dot-dashed curve), however, remaining much smaller than $R_{\omega/\phi}^{OZI}$, namely $R_{\omega/\phi} = 7.5 \cdot \cdot 10$, in agreement with the analysis in [9].

Fig. 8 shows the results of our full calculation of the spin density matrix element ρ_{00} at $\Delta s^{1/2} = 20$ and 100 MeV in the left and right panels, respectively. Near the threshold the meson exchange amplitude behaves as

$$T_{\lambda}^{(M)} \sim \mathbf{k} \cdot [\mathbf{k} \times \boldsymbol{\epsilon}^{*\lambda}]. \quad (48)$$

That means that only $\lambda = \pm 1$ contributes and, therefore, ρ_{00} is suppressed. The pure nucleon s channel amplitude behaves as

$$T_{\lambda}^{(N)} \sim \langle f | \boldsymbol{\sigma} \cdot \boldsymbol{\epsilon}^{*\lambda} | i \rangle, \quad (49)$$

which results in an isotropic spin density, i.e., $\rho_{00} = \rho_{11} = \rho_{-1-1} = 1/3$. The resonance amplitudes have additional terms proportional to $\mathbf{k} \cdot \boldsymbol{\epsilon}^{*\lambda}$, which also enhance ρ_{00} . This effect is seen clearly in the left panel of Fig. 8 for which our qualitative analysis is valid. For ϕ production, where the main contribution comes from the meson exchange channel (cf. Figs. 2 and 5), ρ_{00} is relatively small, $\rho_{00} < 0.05$. But for ω production, where the contribution of the resonance channel is essential, we find $\rho_{00} \sim 0.3$ which is close to an isotropic spin-density distribution with $\rho_{00} \simeq \rho_{11} = \rho_{-1-1} \simeq 1/3$.

Fig. 9 shows the angular distribution of hadronic decays $\phi \rightarrow K^+K^-$ and $\omega \rightarrow \pi^+\pi^-\pi^0$ in $\pi^-p \rightarrow nV$ reactions at $\Delta s^{1/2} = 20$ MeV. The left panel corresponds to a calculation of the vector meson production in forward direction, $0.9 < \cos\theta < 1$, where the cross section achieves a maximum, while the right panel shows its average value in the full angular interval $-1 < \cos\theta < 1$. One can see a striking difference between the ϕ and ω cases: an almost anisotropic distribution for ϕ production ($\mathcal{W} \simeq \frac{3}{2} \sin^2\Theta$) and almost isotropic distribution for ω production ($\mathcal{W} \sim 1$), respectively, which reflect the difference in the corresponding production mechanisms.

A similar difference is predicted for the angular distribution of electrons in $\pi^-p \rightarrow nV \rightarrow ne^+e^-$ reactions shown in Figs. 10 and 11 at $\Delta s^{1/2} = 20$ and 100 MeV, respectively. Again one can see that at $\Delta s^{1/2} = 20$ MeV (Fig. 10) the ϕ and ω cases are very different: an almost anisotropic distribution for ϕ production ($\mathcal{W} \simeq \frac{3}{4}(1 + \cos^2\Theta)$), and almost isotropic distribution for ω production ($\mathcal{W} \sim 1$), respectively. This pronounced difference disappears at $\Delta s^{1/2} = 100$ MeV (Fig. 11).

It should be emphasized that our prediction for the separate decay $\omega \rightarrow e^+e^-$ may be tested experimentally supposed the corresponding detector acceptance is sufficiently large for distinguishing the sharp ω resonance peak in the dielectron invariant mass distribution sitting on the background of the wide ρ^0 meson contribution. Otherwise one should consider the $\omega - \rho^0$ interference as calculated for unpolarized observables in [17]. However, having in mind that the ρ^0 production is a competing channel to the ω production, where the role of the resonances is expected to be even more important because of the larger number of intermediate N^* states, we expect that our prediction of an almost isotropic e^+e^- distribution at invariant mass $M_{e^+e^-} \simeq m_{\omega}$ remains valid in general, reflecting the role of the baryon resonances in the production mechanism.

IV. SUMMARY

In summary we have performed a combined analysis of ω and ϕ production in πN reactions near the threshold at the same energy excess. We find that the meson-exchange amplitude alone can not describe the existing data, rather the role of the direct nucleon term and the nucleon resonance amplitudes is essential. The latter statement is very important

for the ω production, and therefore we investigate the role of nucleon resonances in detail. The ωNN^* couplings as well as the phases of the πNN^* couplings are taken from the recent work [16]. It is found that the resonance contributions can influence significantly the total and the differential cross sections at small energy excess as well as the ratio of the averaged amplitudes of ω and ϕ production. For this ratio we get the value 8.7 ± 1.5 which is much smaller than the value based on the standard OZI rule violation. The dominant contributions are found to stem from the nucleon resonances $N_{\frac{1}{2}-}(1535)S_{11}$, $N_{\frac{1}{2}-}(1650)S_{11}$, and $N_{\frac{1}{2}+}(1440)P_{11}$. However, the other resonances become also important with increasing energy excess.

We have shown that our predictions can essentially be tested by measuring the angular distribution of decay particles in the reactions $\pi N \rightarrow N\phi \rightarrow NK^+K^-$, $\pi N \rightarrow N\omega \rightarrow N3\pi$ and $\pi N \rightarrow NV \rightarrow Ne^+e^-$. Near the thresholds, for the ϕ production we predict an almost anisotropic distribution, while for the ω production an almost isotropic distributions is obtained. Experimentally, this prediction can be tested with the pion beam at the HADES spectrometer at GSI/Darmstadt [38].

It should be stressed that the present investigation is completely based on the conventional meson-nucleon dynamics and, therefore, our predictions may be considered as a necessary background for forthcoming studies of the hidden strangeness degrees of freedom in non-strange hadrons. Finally, it should be emphasized that our study here is a first step from the point of view of a dynamical treatment of the problem, thus going beyond [9]. The main uncertain part is the poor knowledge of the strong cut-off factors for the virtual nucleon and nucleon resonances which are important for the present consideration. Also, the effects of the final state interaction must be investigated which may be pursued by extending the approach of Refs. [12,39].

Acknowledgments

We gratefully acknowledge fruitful discussions with H.W. Barz, R. Dressler, S.B. Gerasimov, L.P. Kaptari, and J. Ritman. One of the authors (A.I.T.) thanks for the warm hospitality of the nuclear theory group in the Research Center Rossendorf. This work is supported by BMBF grant 06DR921, Heisenberg-Landau program, HADES-JINR participation project #03-1-1020-95/2002, and Russian Foundation for Basic Research under Grant No. 96-15-96426.

REFERENCES

- [1] S. Okubo, Phys. Lett. B 5 (1963) 165;
G. Zweig, CERN report No. 8419/TH 412 (1964);
I. Iizuka, Prog. Theor. Phys. Suppl. 37/38 (1966) 21.
- [2] C. Caso et al. (Particle Data Group), Eur. Phys. J. C 3 (1998) 1.
- [3] J. Ellis, M. Karliner, D.E. Kharzeev, M.G. Sapozhnikov, Phys. Lett. B 353 (1995) 319.
- [4] J. Ellis, M. Karliner, D.E. Kharzeev, M.G. Sapozhnikov, Nucl. Phys. A 673 (2000) 256.
- [5] M.P. Locher, Y. Lu, Z. Phys. A 351 (1995) 83;
D. Buzatu, F.M. Lev, Phys. Lett. B 329 (1994) 143.
- [6] J. Gasser, H. Leutwyler, M.E. Sainio, Phys. Lett. B 253 (1991) 252.
- [7] D.B. Kaplan, A.V. Manohar, Nucl. Phys. B 310 (1988) 527;
R.D. McKeown, Phys. Lett. B 219 (1989) 140;
E.M. Henley, G. Krein, S.J. Pollock, A.G. Williams, Phys. Lett. B 269 (1991) 31.
- [8] A.I. Titov, Y. Oh, S.N. Yang, Phys. Rev. Lett. 79 (1997) 1634;
A.I. Titov, Y. Oh, S.N. Yang, T. Morii, Phys. Rev. C 58 (1998) 2429.
- [9] A. Sibirtsev, W. Cassing, Eur. Phys. J. A 7 (2000) 407.
- [10] H.J. Lipkin, Phys. Lett. B 60 (1976) 371.
- [11] G. Fäldt, C. Wilkin, Z. Phys. A 357 (1997) 241;
N. Kaiser, Phys. Rev. C 60 (1999) 057001.
- [12] A.I. Titov, B. Kämpfer, B.L. Reznik, Eur. Phys. J. A 7 (2000) 543.
- [13] B. Friman, H.J. Pirner, Nucl. Phys. A 617 (1997) 496.
- [14] M. Lutz, G. Wolf, B. Friman, Nucl. Phys. A 661 (1999) 526.
- [15] M. Post, U. Mosel, nucl-th/0008040.
- [16] D.O. Riska, G.E. Brown, Nucl. Phys. A 679 (2001) 577.
- [17] M. Soyeur, M. Lutz, B. Friman, nucl-th/0003013.
- [18] M. Post, S. Leupold, U. Mosel, nucl-th/0008027.
- [19] Y. Oh, A.I. Titov, T.-S.H. Lee, Phys. Rev. C 63 025201 (2001) 02520..
- [20] W.S. Chung, G.Q. Li, C.M. Ko, Phys. Lett. B 401 (1997) 1.
- [21] A.I. Titov, B. Kämpfer, V.V. Shklyar, Phys. Rev. C 59 (1999) 999.
- [22] K. Nakayama, A. Szczurec, C. Hanhart, J. Haidenbauer, J. Speth, Phys. Rev. C 57 (1998) 1580.
- [23] K. Nakayama, J.W. Durso, J. Haidenbauer, C. Hanhart, J. Speth, Phys. Rev. C 60 (1999) 055209.
- [24] F. Balestra et al. (DISTO Collaboration), Phys. Rev. Lett. 81 (1998) 4572; Phys. Lett. B 468 (1999) 7;
R. Dressler et al. (DISTO Collaboration), in Annual Report 2000 of the Institute of Nuclear and Hadron Physics.
- [25] Aachen-Berlin-Hamburg-Heidelberg-München Collaboration, Phys. Rev. 175 (1968) 1669.
- [26] J.D. Bjorken, S.D. Drell, *Relativistic quantum mechanics*, McGraw-Hill Inc., 1964.
- [27] R. Machleidt, Adv. Nucl. Phys. 19 (1989) 189.
- [28] H. Haberzettl, Phys. Rev. C 56 (1997) 2041;
H. Haberzettl, C. Bennhold, T. Mart, T. Feuster, Phys. Rev. C 58 (1998) 40.
- [29] C. Itzykson, J.-B. Zuber, *Quantum Field Theory*, McGraw-Hill, Inc., Singapore, 1985

- [30] A.I. Titov, T.-S.H. Lee, H. Toki, O. Streltsova, Phys. Rev. C 60 (1999) 035205 .
- [31] Th.A. Rijken, V.G.J. Stoks, Y. Yamamoto, Phys. Rev. C 59 (1999) 21.
- [32] T. Sato, T.-S.H. Lee, Phys. Rev. C 54 (1996) 2660.
- [33] A. Waluyo, C. Bennhold, H. Haberzettel, G. Penner, U. Mosel, T. Mart, nucl-th/0008023.
- [34] U.-G. Meissner, V. Mull, J. Speth, J.W. Van Orden, Phys. Lett. B 408 (1997) 381.
- [35] Landolt-Börnstein, New Series **I/12**, A. Baldini et al. *Total cross sections of high energy particles*, Springer-Verlag, 1988.
- [36] H. Karami et al. Nucl. Phys. B 154 (1979) 503.
- [37] C. Hanhart, A. Kudryavtsev, Eur. Phys. J. A 6 (1999) 325.
- [38] J. Friese et al. (HADES collaboration), GSI report 97-1, p. 193 (1997).
- [39] K. Schilling, F. Storim, Nucl. Phys. B 7 (1968) 559.

TABLES

baryon	M_{N^*}	$f_{\pi NN^*}$	$g_{\omega NN^*}$	$\Gamma_{N^*}^0$	$B_{N^*}^\pi$
$N_{\frac{1}{2}}^{1+} N$	940	1.0	10.35	—	—
$N_{\frac{1}{2}}^{1+} P_{11}$	1440	0.39	6.34	350	0.65
$N_{\frac{3}{2}}^{3-} D_{13}$	1520	-1.56	8.88	120	0.55
$N_{\frac{1}{2}}^{1-} S_{11}$	1535	0.36	-5.12	150	0.45
$N_{\frac{1}{2}}^{1-} S_{11}$	1650	0.31	2.56	150	0.73
$N_{\frac{5}{2}}^{5-} D_{15}$	1675	0.10	10.87	150	0.45
$N_{\frac{5}{2}}^{5+} F_{15}$	1680	-0.42	-14.07	130	0.65
$N_{\frac{3}{2}}^{3-} D_{13}$	1700	0.36	2.81	100	0.10
$N_{\frac{3}{2}}^{3-} P_{13}$	1720	-0.25	-3.17	150	0.15

TABLE I. Parameters for the resonance masses, coupling constants, total decay widths and branching ratios for $N^* \rightarrow N\pi$ decays. The resonance masses and decay widths are in units of MeV.

FIGURES

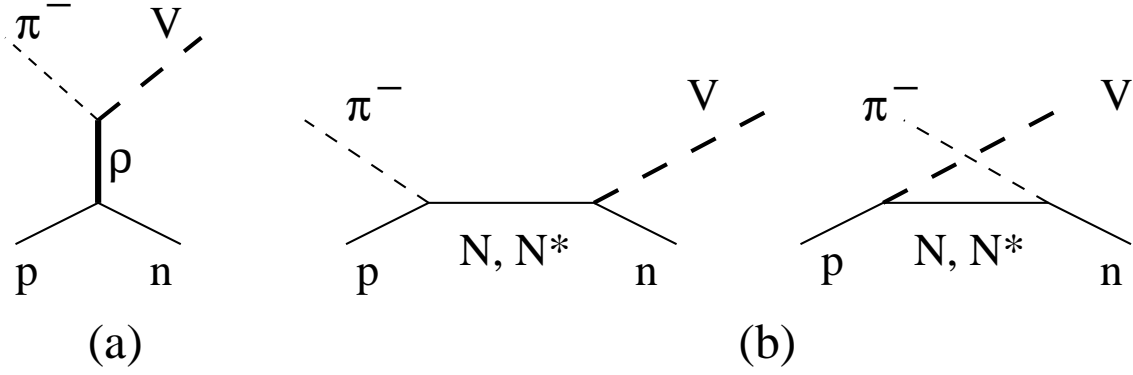


FIG. 1. Diagrammatic representation of the $\pi^- p \rightarrow V n$ reaction mechanisms with $V = \omega, \phi$. (a) meson exchange diagram with vector meson emission from the $V\rho\pi$ vertex, (b) nucleon and nucleon-resonance vector-meson production in the VNN and VNN^* vertices.

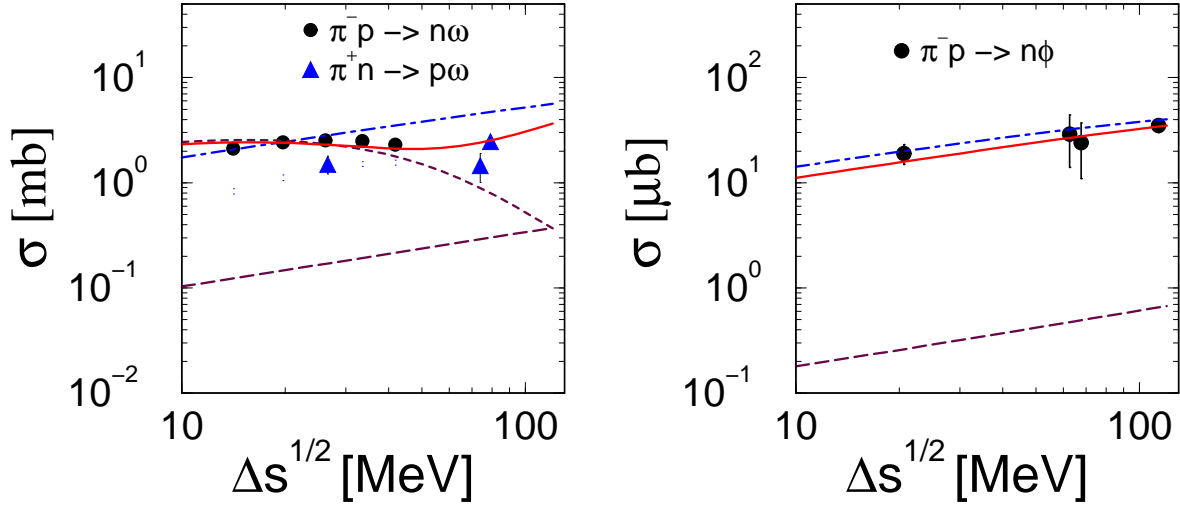


FIG. 2. Total cross sections for the reactions $\pi N \rightarrow N\omega$ (left panel) and $\pi^- p \rightarrow n\phi$ (right panel) as a function of the energy excess $\Delta s^{1/2}$. The meaning of the curves is: meson exchange - dot-dashed, direct and crossed nucleon terms - long-dashed, N^* resonances - dashed, full amplitude - solid. Data from [35,36].

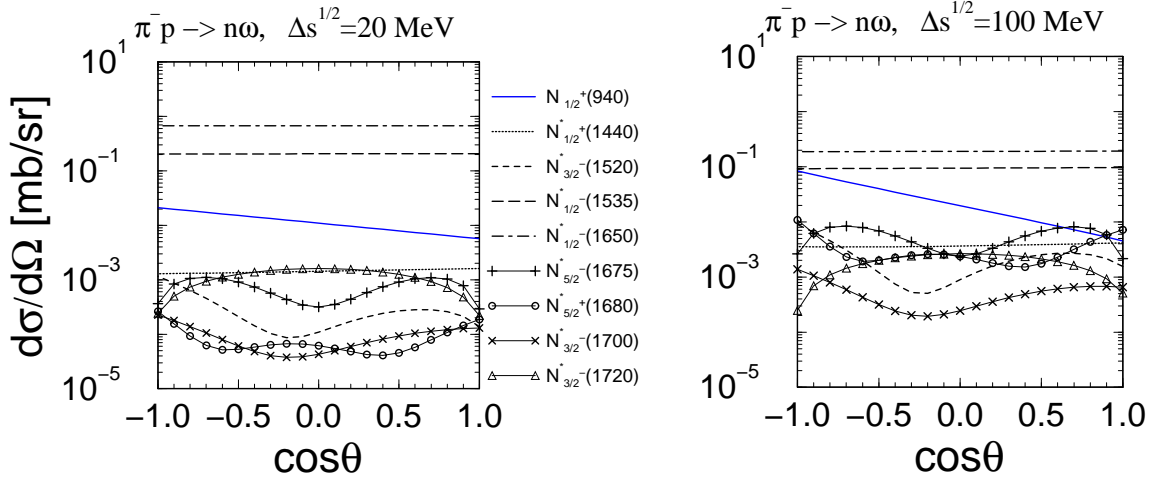


FIG. 3. Individual contributions of nucleon resonances listed in Table 1 to the angular differential cross section of ω production at $\Delta s^{1/2} = 20$ MeV (left panel) and 100 MeV (right panel).

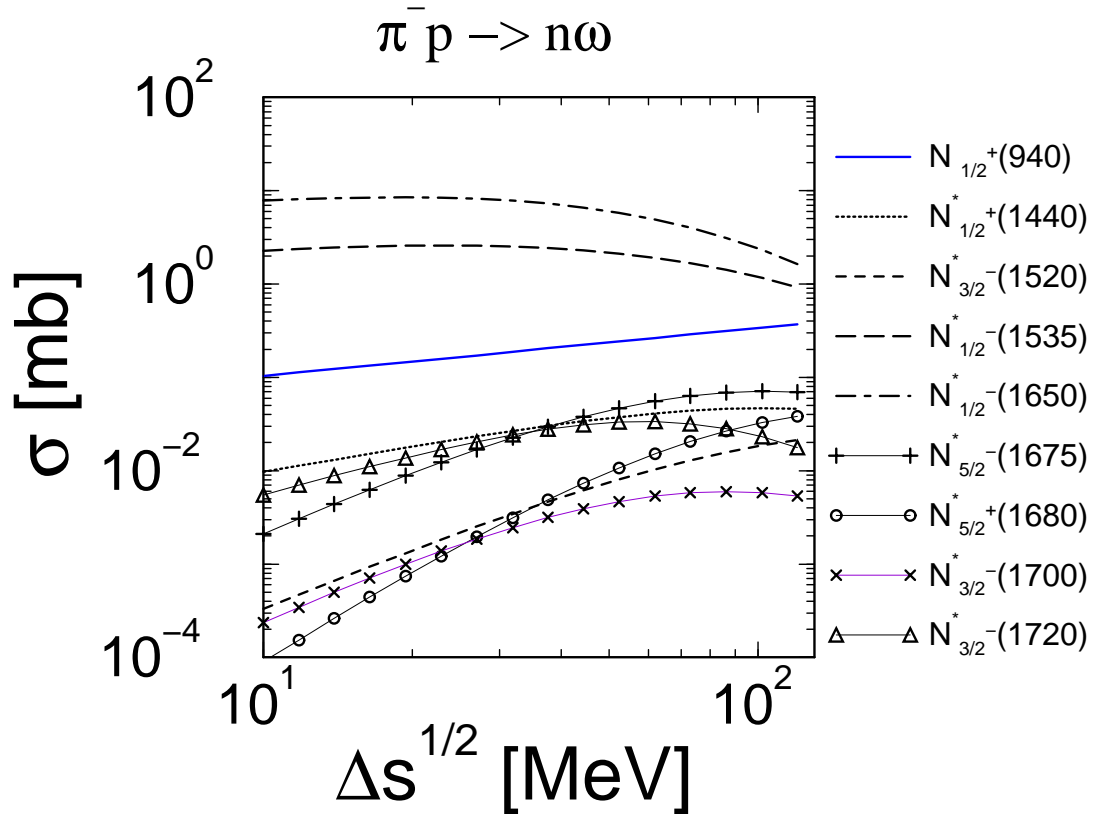


FIG. 4. Individual contributions of nucleon resonances listed in Table 1 to the total cross section of ω production as a function of $\Delta s^{1/2}$.

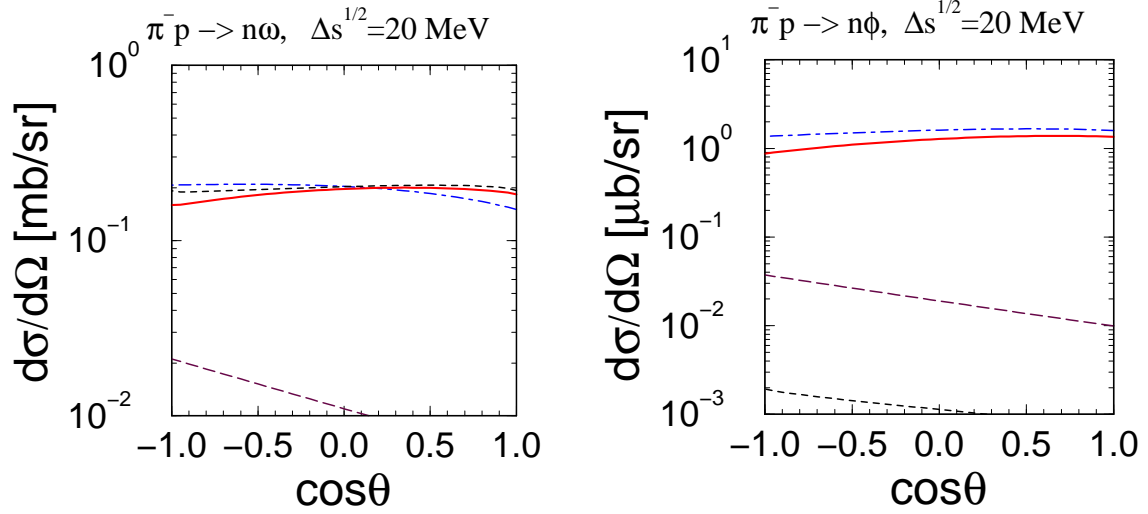


FIG. 5. Angular differential cross sections for the reactions $\pi^- p \rightarrow n\omega$ (left panel) and $\pi^- p \rightarrow n\phi$ (right panel) at $\Delta s^{1/2} = 20 \text{ MeV}$. Notation as in Fig. 2.

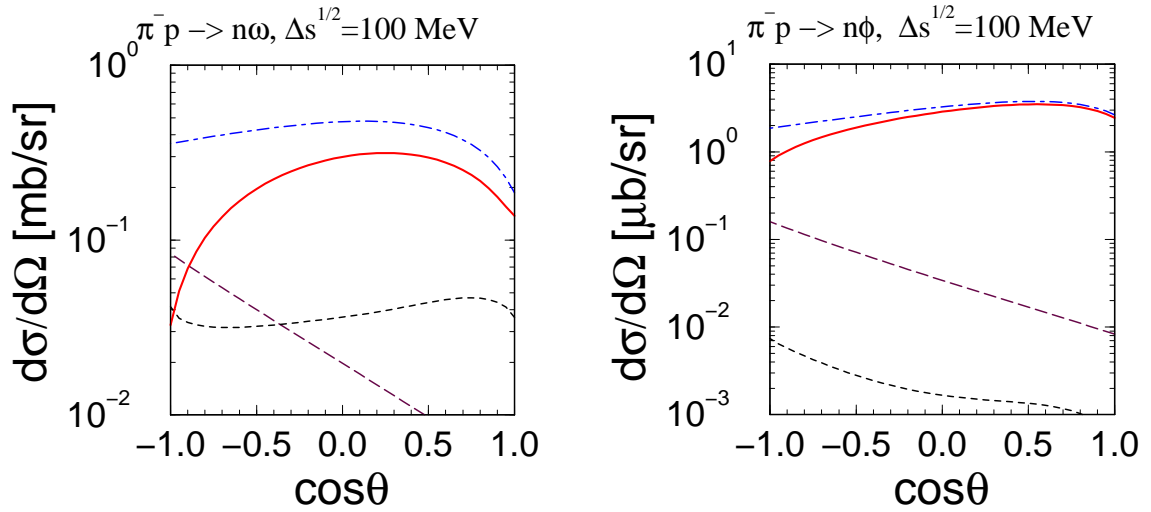


FIG. 6. As in Fig. 5 but at $\Delta s^{1/2} = 100 \text{ MeV}$.

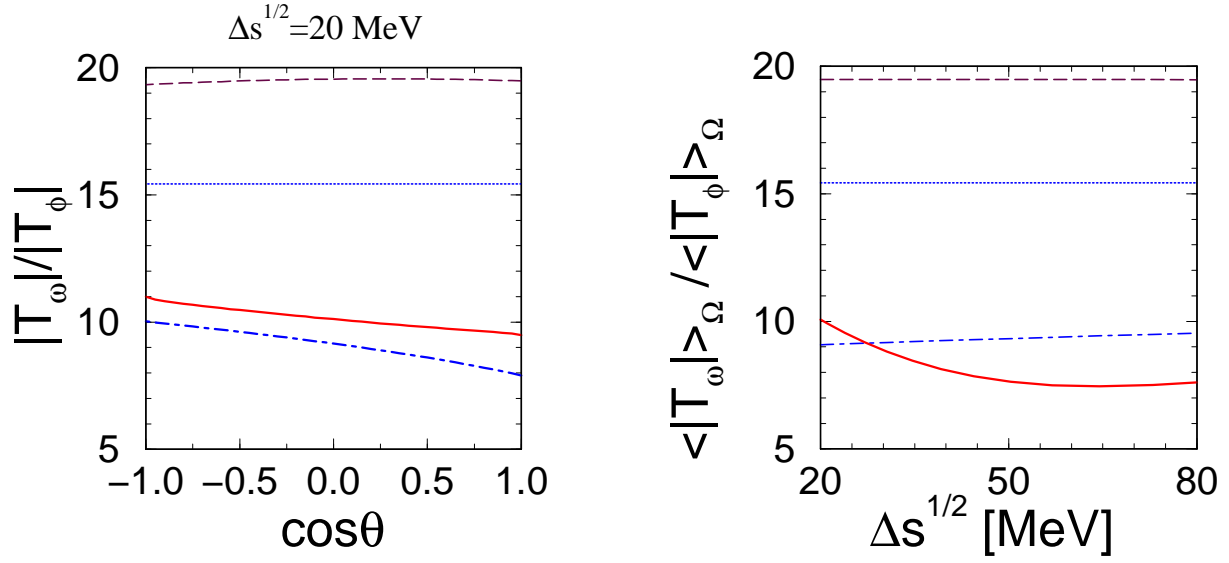


FIG. 7. Ratio of the amplitudes of ω and ϕ production. Left panel: the ratio as a function of $\cos\theta$ at $\Delta s^{1/2} = 20 \text{ MeV}$, right panel: the ratio averaged over production angle as a function of $\Delta s^{1/2}$. Notation as in Fig. 2.

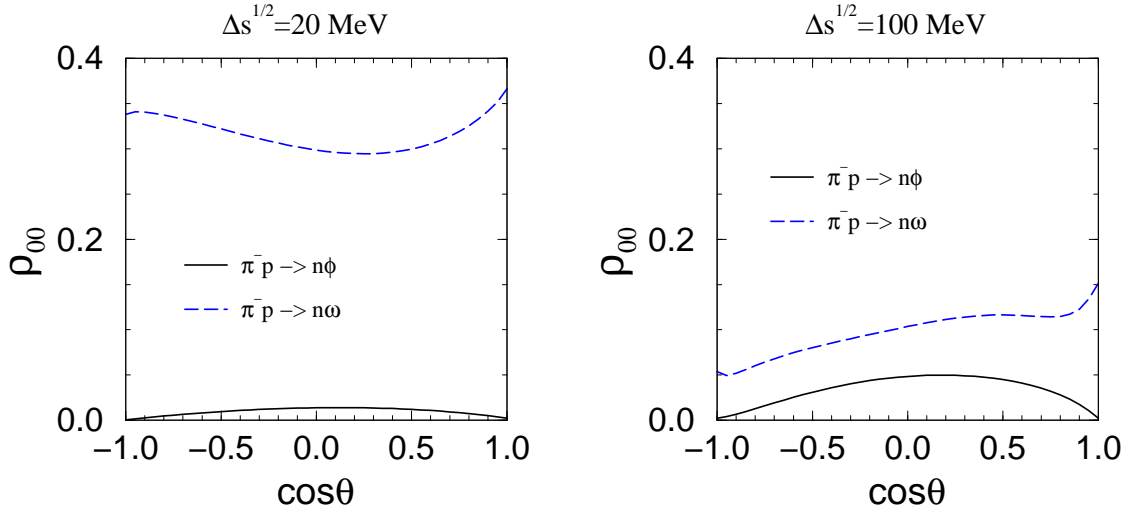


FIG. 8. Spin-density matrix element ρ_{00} for ω and ϕ production as a function of $\cos\theta$ at $\Delta s^{1/2} = 20 \text{ MeV}$ (left panel) and 100 MeV (right panel).

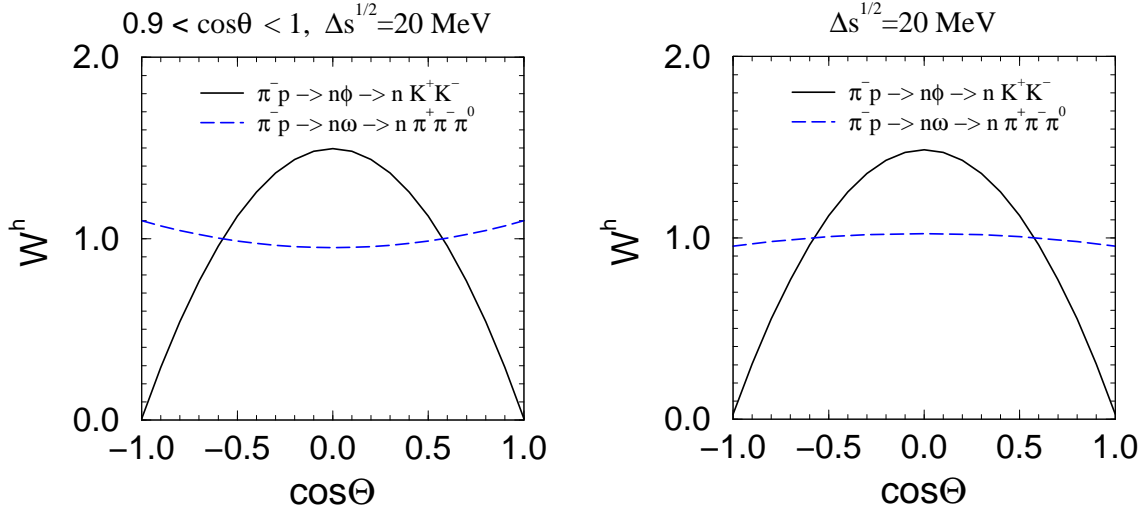


FIG. 9. Meson angular distributions in the reactions $\pi^-p \rightarrow n\phi \rightarrow nK^+K^-$ and $\pi^-p \rightarrow n\omega \rightarrow n\pi^+\pi^-\pi^0$, at $\Delta s^{1/2} = 20$ MeV. Left panel: the distribution at forward vector meson production angles, right panel: the distribution averaged over all production angles.

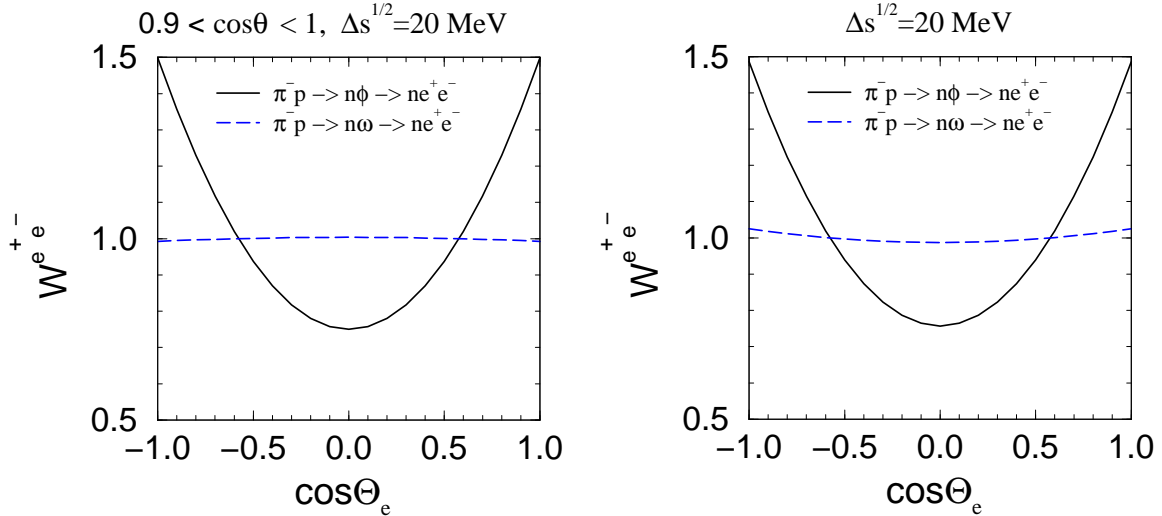


FIG. 10. Electron angular distributions in the reaction $\pi^-p \rightarrow nV \rightarrow ne^+e^-$ at $\Delta s^{1/2} = 20$ MeV. Left panel: the distribution at forward vector meson production angles, right panel: the distribution averaged over the all production angles.

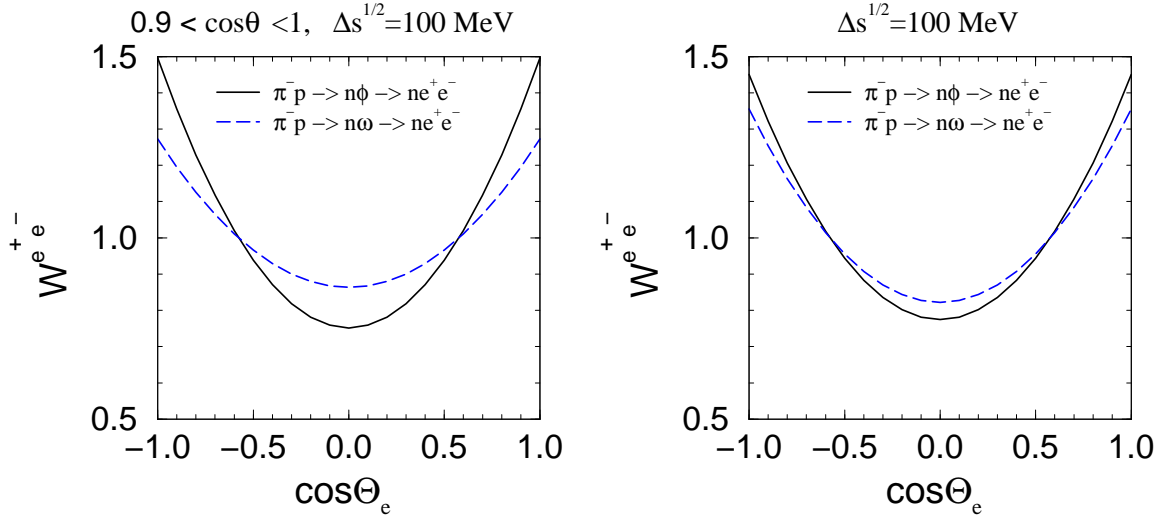


FIG. 11. The same as in Fig. 10 but at $\Delta s^{1/2} = 100$ MeV.